Hindawi
Geofluids
Volume 2022, Article ID 9125283, 17 pages
https://doi.org/10.1155/2022/9125283

Research Article

Experimental Study on Shield Tunneling Control in Full Section Water-Rich Sand Layer of Collapsible Loess

Yuan Mei,[1,2] Xinyue Zhang,[1,2] Shumin Zhang,[1,2] Rong Wang,[1,2] Tong Yang,[1,2] and Yuhang Zhang[1,2]

[1]*College of Civil Engineering, Xi'an University of Architecture and Technology, Xi'an, Shaanxi 710055, China*
[2]*Shaanxi Key Laboratory of Geotechnical and Underground Space Engineering, Xi'an University of Architecture and Technology, Xi'an, Shaanxi 710055, China*

Correspondence should be addressed to Xinyue Zhang; zhangxy@xauat.edu.cn

Received 20 April 2022; Revised 8 August 2022; Accepted 8 August 2022; Published 28 August 2022

Academic Editor: Di Feng

Taking China's first application of domestic shield tunneling in a water-rich sand layer for crossing a high-speed railway as research background, the influence of changes in the shield tunneling parameters on ground settlement is analyzed based on field tests, and a construction control method suitable for shield tunneling under a risk source in a water-rich sand layer is proposed. The test results show that the use of 10% sodium bentonite as the soil modifier for soil pressure balance shield tunneling into the water-rich sand layer has advantages, while adding 50% loess into the bentonite slurry in the gravel sand layer can greatly improve the impermeability of the soil; the settlement of soil can be effectively reduced by using the special segment with grouting holes for deep grouting and applying the adaptive transformation of the shield cutter. Based on the statistical analysis results, a reasonable range for the cutter head torque, cutter head speed, chamber pressure, bentonite injection volume, and advanced speed in the water-rich sand layer can provide a construction control basis for similar projects and provide data support for the compilation of relevant specifications.

1. Introduction

During the application of EPB shield in water rich sand layer, the determination of shield tunneling parameters is very challenging due to the problems such as low arched efficiency of surrounding rock, high pore pressure, and easy collapse of tunnel working face [1–3]. If the construction parameters are set improperly, it is difficult to ensure the safety of the existing structure when the shield machine needs to pass through major risk sources. Especially when the shield machine passes through the railway in operation, if the ground settlement and track deformation are not properly controlled, it will pose a great threat to the safe operation of the existing railway [4]. However, at present, there are few research results on shield construction process control in such stratum, and there is no effective construction control method to control the settlement within the limits required by the current standard.

Some scholars have studied the characteristics of ground settlement caused by shield tunnels in adverse strata. In the soft clay layer, the volume loss caused by shield tunneling is mostly between 0.5% and 2.0%. Compared with the settlement-sensitive area in Shanghai, the volume loss caused by tunnel construction in the newly reclaimed land area of Hong Kong is likely to be larger, but the operation of shield machine drivers has a great impact on the settlement, which is not easy to predict [5–7]. Therefore, it is very important to determine a reasonable range of shield tunneling parameters. The change in construction parameters also has a certain impact on surface settlement. For collapsible loess strata, compared with the filling rate of grouting, changes in the eccentricity ratio and support pressure ratio of the shield are more likely to cause surface heave and subsidence [8]. Lin et al. [9] also studied the stress redistribution and soil arch evolution caused by EPB shield tunneling in the sand, determined the boundary between the soil arch

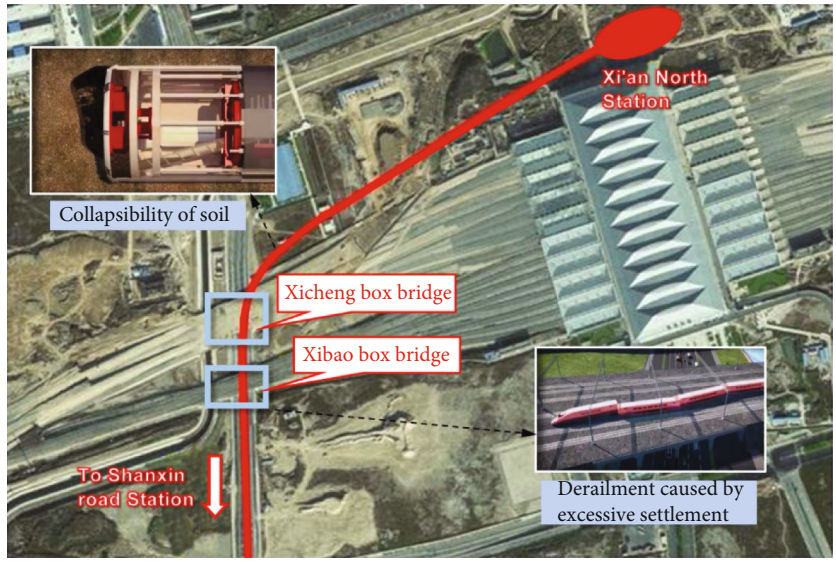

Figure 1: The relationship for the location of Metro Line 4 passing through two box bridges.

area and the loose area, and demonstrated the three-dimensional stress transfer mechanism in the soil arch area. In the framework of particle thermodynamics, Bai et al. [10, 11] established a new thermal hydro mechanical coupling mechanism for particle rearrangement of saturated/unsaturated soils. The model can effectively reflect the influence of saturation, temperature, and phase change on soil deformation. Sohaei et al. [12] carried out several small three-dimensional model tests to simulate the volume loss during shield tunneling and found that increasing the relative density of sand can reduce the surface settlement caused by tunnel construction. Some scholars have improved and innovated construction methods to control the surface settlement caused by shields in adverse strata. Ye et al. [13], Lai et al. [14], and Chen et al. [15] proposed the construction methods of the double-O-tube (DOT) tunneling method in soft soil, sleeve valve pipe grouting for pre-reinforcement and I-steel support for portals in loess areas, rectangular shafts, and MJS columns to reinforce the sand under the existing double tunnel to reduce settlement. Wang et al. [16] reduced the settlement caused by a tunnel beneath a bridge by adding a U-shaped structure under the bridge as the expansion foundation of the raft foundation. Yuan et al. [17, 18] reinforced granite residual soil with glass fiber and (SH polymer). The micro-interaction mechanism and impact resistance of the added solid samples were studied by SEM and drop weight tests. The research shows that the reinforcement technique has good application effect. Li et al. [19] adopted pile foundation underpinning technology to transfer the overlying load of the bridge foundation group to new underpinning piles, which eliminated the obstacles in front of the proposed tunnel, provided conditions for shield construction, and ensured the safe use of expressways above the tunnel.

With the development of urban rail transit, an increasing number of tunnel projects need to cross existing railway lines. The interaction between railway train operation and shield tunneling will lead to additional settlement of railways [20]. Therefore, it is necessary to control the risk of tunnel construction. Zhao et al. [21] determined that grouting curtain measures are the best reinforcement scheme for shield tunneling under a railway bridge through a three-factor and four-level model based on the principle of the orthogonal experiment. Qian et al. [22] analyzed the surface settlement characteristics of a tunnel passing through a high-speed railway at different angles in terms of the ground settlement trough, stratum slip line, and track irregularity to provide technical support for the safety evaluation of tunnel crossing high-speed railway projects. Zheng et al. [23] used the multistage regulation strategy to control the settlement of the construction of two overlapped tunnels under an existing line and successfully controlled the ground settlement along the railway by continuously adjusting the shield tunneling parameters.

However, due to the complexity of geological conditions, there are few studies on settlement control methods for shield tunneling under risk sources in water-rich sand layers. Numerical simulation seems to be an appropriate tool to control the driving parameter variables and verify the effect of settlement control measures [24–26]. However, due to the complex construction conditions in the tunnel section and numerous shield tunneling parameters, the results of numerical model calculations are often not ideal and inconsistent with the field monitoring results. To ensure the safety of operating railways during tunnel construction, a section in front of a railway box bridge is set as a test zone for a field test. According to the feedback of the field response during construction, a settlement control method suitable for adverse strata is proposed, and the influence of the driving parameters on the surface settlement is analyzed. Based on the statistical test results, a reasonable range of driving parameters when the shield underpasses the risk source in the water-rich sand layer is proposed, which can provide a reference for similar projects in the future.

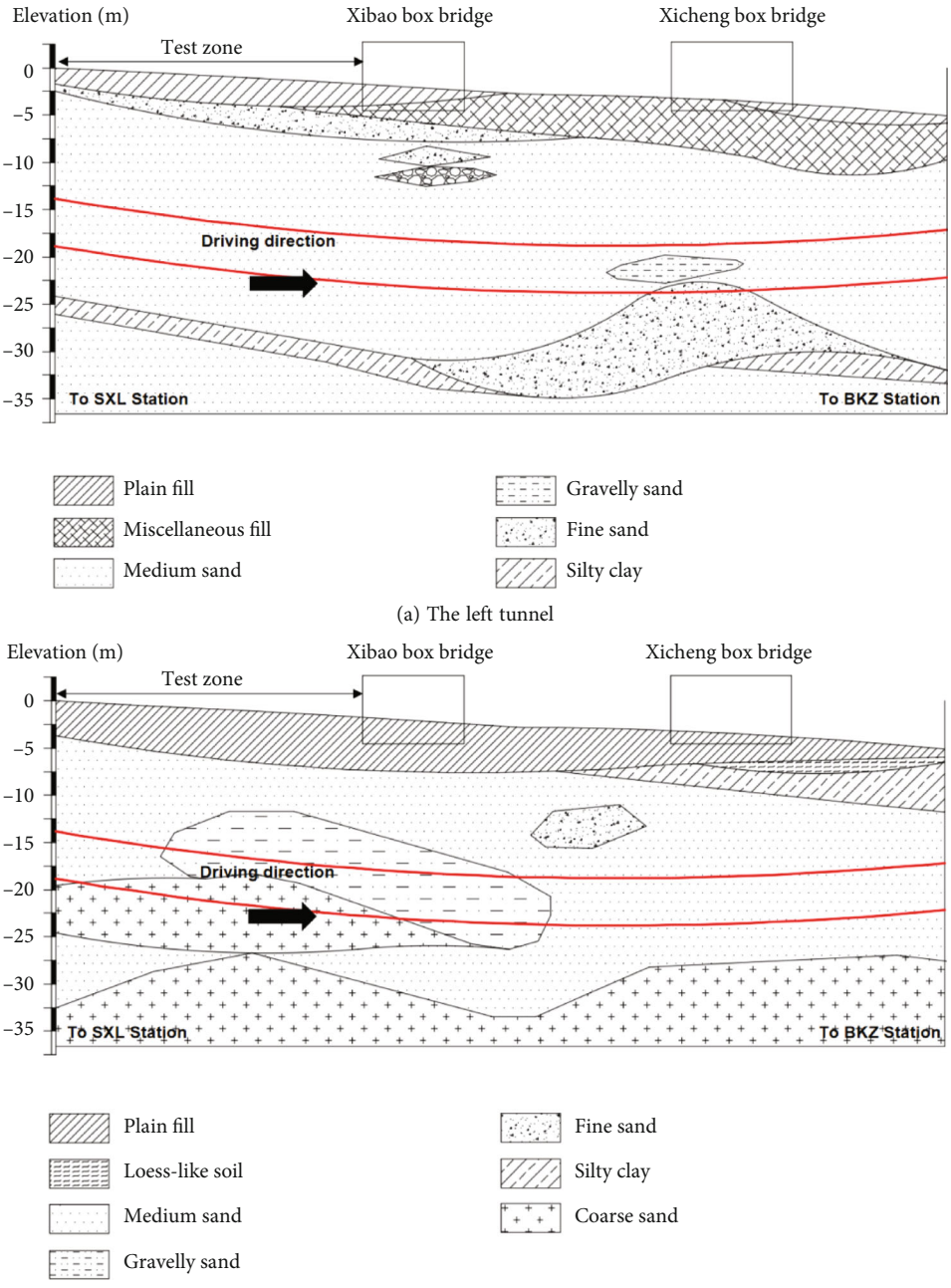

Figure 2: Longitudinal profile of the tunnels, the box bridges and geological conditions.

2. Research Background

2.1. Project Overview. The section of Xi'an Metro Line 4 from Shangxin Road station to North Railway Station is constructed by shield tunneling, which passes under the box bridges of the Xibao passenger dedicated line and the Xicheng passenger dedicated line. This is the first time that the construction of an undercrossing high-speed railway line has been carried out in a full section of water-rich sand in China. The proposed section tunnel has large surface vehicle flow and heavy traffic, there are many existing buildings on both sides of the line, and there are many underground pipelines nearby, so it is necessary to strictly control the vertical displacement of the track. The railway track above the tunnel is the ballasted track. According to the provisions of the Code for Design of Railway Earth Structure (TB 10001-2016), to ensure the safe operation of the railway, the cumulative vertical displacement of the ballasted track should be controlled within ±10 mm for each single track tunnel.

The relationship for the location of Metro Line 4 passing through the box bridges of the Xibao passenger dedicated line and Xicheng passenger dedicated line is shown in Figure 1. The intersection angle of the left and right tunnels with the Xicheng box bridge and Xibao box bridge is

Table 1: Physical and mechanical parameters of the soil layer.

Soil name	Dry density ($g \cdot cm^{-3}$)	Water content (%)	Compression modulus (MPa)	Cohesion (kPa)	Internal friction angle (°)	Standard penetration
Plain fill	1.58	20.4	—	22	15	9
Miscellaneous fill	1.75	—	—	5	10	—
Loess-like soil	1.63	20.4	9.4	35	23	19
Medium sand	1.57	16.1	14.6	0	32	64
Gravelly sand	1.96	20.1	15.7	0	33	60
Fine sand	1.65	18.7	15.7	0	31	44
Silty clay	1.61	24.7	5.3	33	18	26
Coarse sand	1.63	17.3	13.8	0	34	—

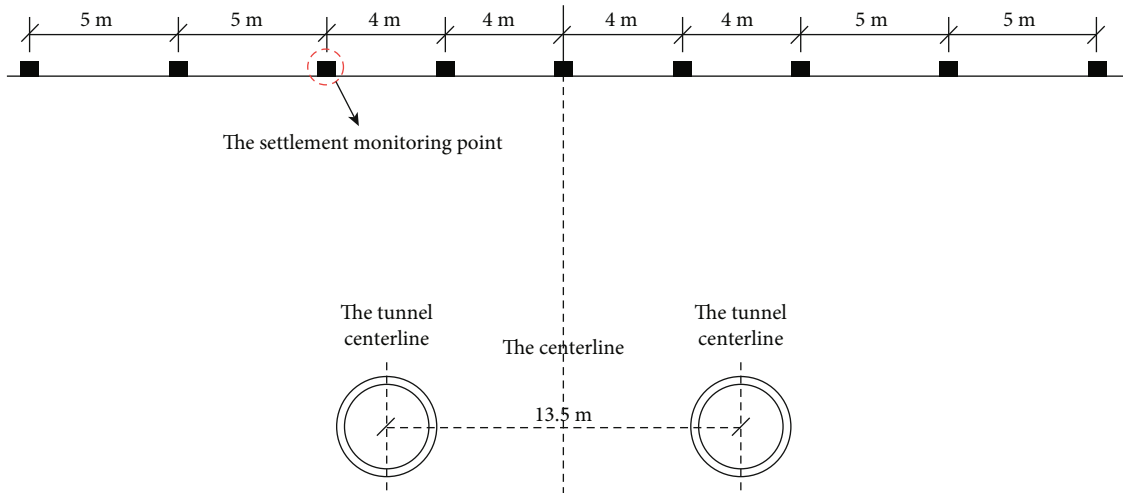

Figure 3: Layout of the surface settlement monitoring points in the test zone.

approximately 70°, and the two box bridges are four-hole box structures with a height of 9.8 m. The width of the Xibao box bridge is 41 m, the width of the Xicheng box bridge is 70.75 m, and the distance between the two box bridges is 78.95 m. The excavation diameter of the shield machine is 6.28 m, and the outer diameter of the segment is 6 m.

2.2. Geological Conditions. According to the field investigation report, the geological section of the section crossed by Xi'an Metro Line 4 and the location relationship between the section and the railway box bridges are shown in Figure 2. The overburden soil thickness of the left and right tunnels is approximately 18 m, which is mainly composed of plain fill, miscellaneous fill and medium sand. The soil layer under the two box bridges is sand, which consists of medium sand, coarse sand, and gravel sand. The unfavorable stratum in the site is loess-like soil, belonging to collapsible loess, but its content is lower, and the impact on the interval is also small. The main aquifers are the Holocene alluvial medium sand layer, coarse sand layer, and the lens of the Middle Pleistocene silty clay sand layer. The three soil layers have good water permeability and high water content. The Holocene alluvial medium sand layer and coarse sand layer are widely distributed. The lens of the Middle Pleistocene silty clay sand layer is distributed discontinuously.

The geological condition parameters of typical strata are shown in Table 1. The soil in the tunnel contour line of the whole project is sandy soil with a large SPT value and high density, and all of them are located below the normal groundwater level with a high permeability coefficient. The water content of sand has a significant impact on the surface settlement [27], and the construction risk is high when tunneling in this kind of dense water-rich sand layer. On the one hand, the driving speed is slow; on the other hand, it is difficult to establish the pressure balance of the earth chamber of the shield machine, and the arching effect is poor, which easily causes the heading face to collapse. If the surface settlement or track deformation exceeds the limit value of the specification, it is difficult to guarantee the construction safety of shield tunneling through culverts and the operation safety of existing railways.

3. Field Test

3.1. Test Zone Setting and Monitoring Scheme. To analyze the influence of driving parameters on surface settlement

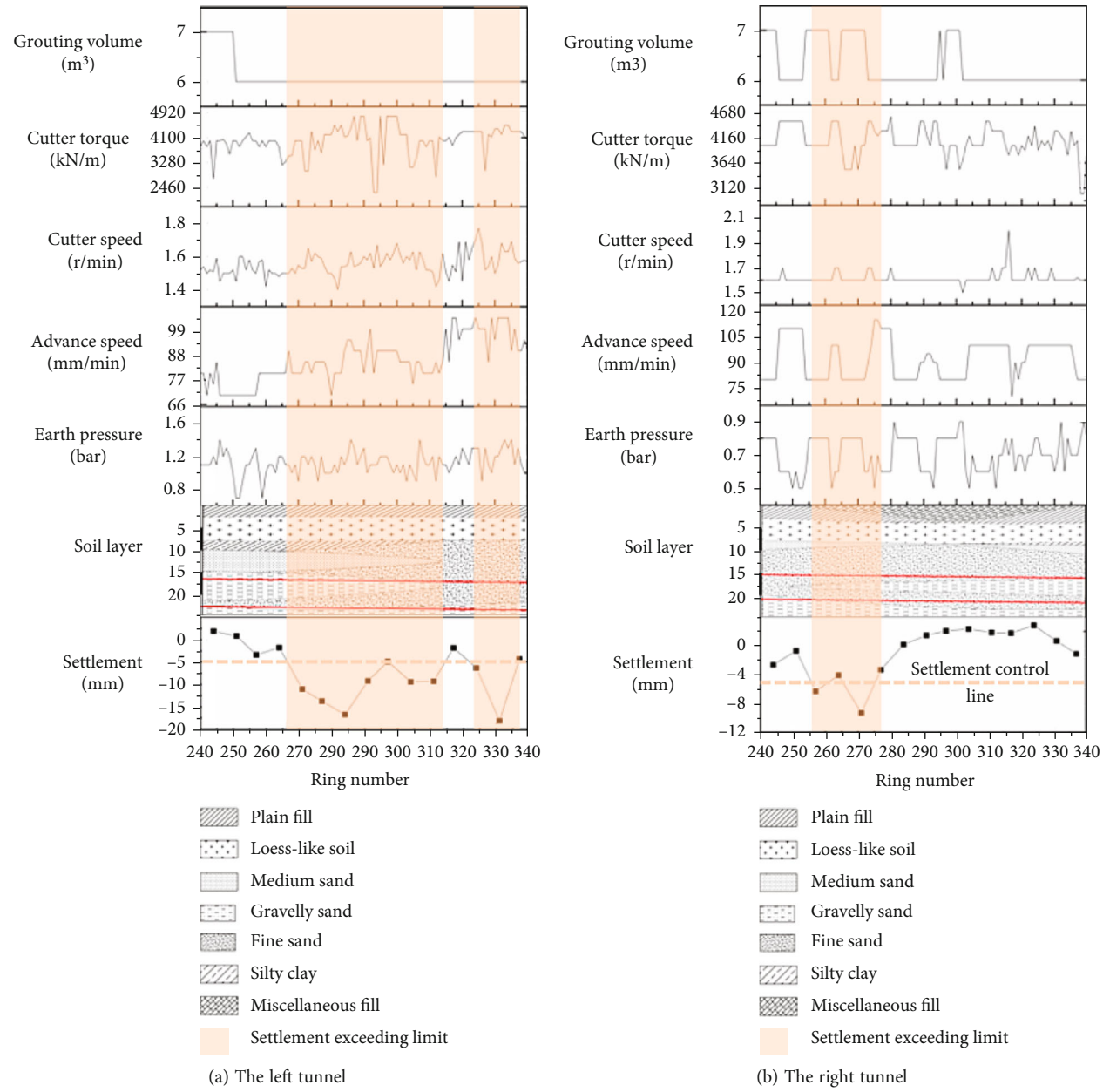

Figure 4: The driving parameters and the surface settlement in the test zone.

when the shield machine passes through a dense water-rich sand layer, an area with a length of 150 m before the shield machine passes through two box bridges is set as the test zone for the field test (as shown in Figure 2). Similar ground conditions ensure the similarity of the ground settlement response between the test zone and the zone under the railway. When shield tunneling is performed in the test zone, the advance speed, cutter head speed, cutter head torque, chamber pressure, and other driving parameters of the shield machine are recorded, and appropriate monitoring points are set in the test zone to monitor the ground settlement to provide the basis for the design and optimization of the driving parameters when the shield passes through two box bridges. The horizontal layout of the monitoring points in the test zone is shown in Figure 3. The monitoring points are arranged symmetrically along the central line of the double-line tunnels, with spacings of 4 m and 5 m in turn. A monitoring section is set every 10 m along the forward direction of the tunnel centerline, and the surface settlement monitoring point is buried in the undisturbed soil at a depth of 10 cm. The settlement points are monitored by the first-class settlement levelling measurement. DSZ2 level + indium steel ruler is used as the monitoring instrument, and the reading height difference of each monitoring point is required to be controlled not to exceed ±0.3 mm.

3.2. Statistics of the Shield Driving Parameters. As shown in Figure 4(a), during the process of shield tunneling through

the test zone, the left line tunnel was first excavated in the soil layer with more gravelly sand. From ring 250, the ground settlement over the left line tunnel increased rapidly, possibly due to a sudden drop in the chamber pressure, and the stratum was sensitive to changes in pressure. Due to the poor flow plasticity of the sand layer soil, the friction resistance between the sand particles is large, and the SPT blow count of the sand layer in this zone is high, so the sand layer is quite dense. When the cut sand fills the soil bin and screw machine, the cutter head torque increases, which directly reduces the advance speed. At the same time, the decrease in the amount of grouting at ring 250 also aggravates the increase in surface settlement, and the settlement reaches −16.7 mm when shield tunneling reaches ring 285. Then, with the decrease in the cutter head torque and the gradual stabilization of the chamber pressure, the driving speed is also improved, and the surface settlement is gradually reduced, which is controlled within −10 mm. When reaching ring 330, the ground settlement suddenly increases to −18.1 mm, the torque and rotation speed of the cutter head decrease, and the driving speed increases. Excessive excavation speed can easily lead to aggravation of the surface settlement. Therefore, when the shield goes under the railway box bridge with strict settlement control requirements, the tunnelling speed should be reduced to ensure the safe operation of the railway.

When the right line tunnel is driven, as shown in Figure 4(b), the fluctuation range of the chamber pressure and advance speed in the whole test zone is wide, and the parameter control is not ideal. The fluctuation of surface settlement is relatively large between ring 240 and ring 270. After entering ring 270, the fine silt in front of the shield tunnel decreases, the gravelly sand increases gradually, and the surface subsidence increases rapidly. This is mainly because the increase of large soil particle content in the stratum leads to the decrease of the stratum's resistance to deformation [28]. Under the condition that the mixing ratio of foaming agent, bentonite, and other materials injected into the shield machine excavation surface is not applicable to the stratum, the disturbance degree and range of the ground displacement and pore water pressure on the excavation surface are significantly increased, resulting in large surface settlement. Therefore, the stability of the water rich sand layer in this area should be improved by studying the properties of the gravelly sand and adjusting the slurry concentration.

Through the monitoring of the surface settlement of the test zone, it is found that the settlement value of many monitoring points is more than 10 mm and the maximum settlement value is −18.1 mm. If the shield machine still performs the construction of the tunnel under the box bridges according to these driving parameters, the surface settlement will not be smaller than the limit value required by the specification, thus causing a substantial threat to the operating railway above. In addition, there are few studies on the soil improvement of shield tunnels in water-rich sand layers [29, 30], and the parameters are often set according to engineering experience, which directly affects the success or failure of the project. Obtaining a suitable soil conditioner for a water-rich sand layer is also a difficult problem. Therefore, based on the statistics and analysis of the driving parameters and ground settlement values in the test zone, a series of optimization control measures are proposed to ensure the safety and stability of shield tunneling under railway box bridges.

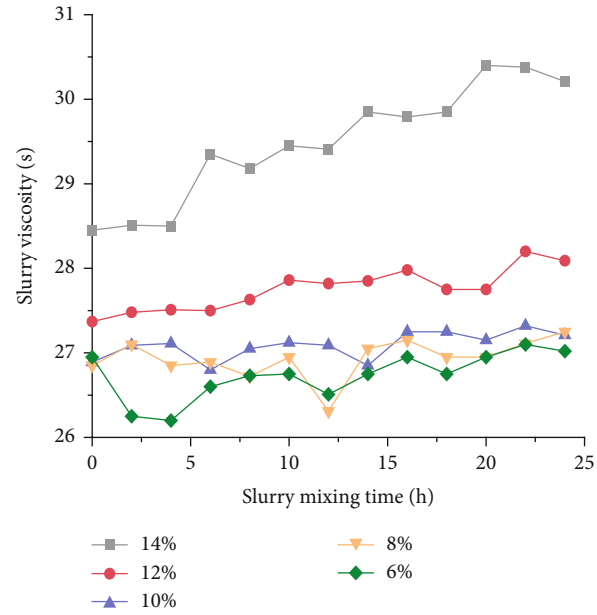

Figure 5: Time dependence curve of the slurry viscosity.

4. Settlement Control Methods of Shield Construction in a Water-Rich Sand Layer

4.1. Soil Improvement Agent and Its Proportion. The soil improvement agent can strengthen the working face of the formation by filling and bonding the original porous medium with its improved slurry. In the practical application process, the diffusion and flow of slurry also need to consider the influence of medium heat transfer coefficient, groundwater level fluctuation, and other factors. Existing studies have shown that the heat transfer coefficient and water level change of porous media will have an impact on the migration of soil particles and the formation stiffness [17, 18, 31]. Therefore, it is necessary to focus on the design of bentonite slurry improvement test to ensure that the soil improvement effect in the water rich sand layer meets the settlement control requirements of the shield tunnel under the railway box bridge. First, through engineering experience, different concentrations of sodium bentonite slurry were prepared for the expansion test, and the viscosity curve of bentonite slurry with time is shown in Figure 5. When the addition ratio of bentonite is less than 10%, the increase in slurry viscosity with mixing time is not obvious. When the addition ratio of bentonite is greater than or equal to 10%, the slurry viscosity increases with increasing bentonite addition and mixing time. Considering the economy of the project, sodium bentonite with an expansion time of 18 h and a concentration of 10% was selected as the modifier.

Combined with engineering experience and relevant research, the permeability of sand has an important relationship with the particle size and composition of solid

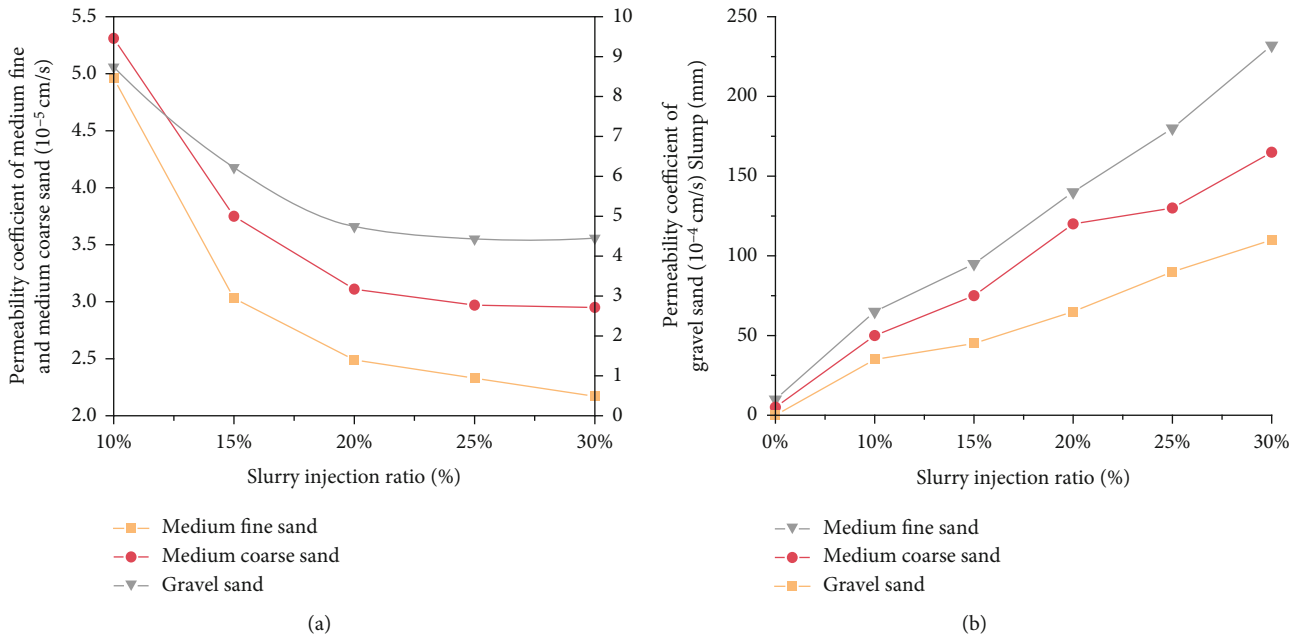

Figure 6: (a) Relation curve of the slurry injection ratio and the permeability coefficient. (b) Relation curve of the slurry injection ratio and the slump.

Table 2: Test results for improving gravel sand with bentonite and loess mixed mud.

Mass ratio of loess to bentonite	Permeability coefficient (cm/s)	Slump (mm)
1 : 3	1.83×10^{-4}	110
2 : 3	6.36×10^{-5}	120
3 : 3	3.47×10^{-5}	160

components [10, 11], and the different injection ratio of slurry will lead to the change of solid components. Therefore, it is necessary to set different mud injection ratios for testing and determine the permeability coefficient and slump of various improved sands to determine the optimal injection ratio. The test results are shown in Figure 6. As shown in Figure 6, the impermeability of the improved soil is obviously improved after adding bentonite mud. When the mud injection ratio exceeds 20%, the increase in sand impermeability gradually slows with increasing mud injection quantity. Therefore, considering the economy and improvement effect, the mud injection ratio is set to 20%. At this time, the slump of medium fine sand and medium coarse sand is between 100 and 150 mm, which meets the requirements of the optimal slump of shield construction ballast soil, and the permeability coefficient reaches the order of 10^{-5} cm/s. However, for gravel sand, the slump is only 65 mm at this time, and the improved permeability coefficient is not ideal, which only reaches the order of 10^{-4} cm/s. Therefore, it is necessary to find a more suitable modifier for gravel sand in combination with engineering applications.

Combined with the widespread distribution of loess in the Xi'an area, gravelly sand is improved by adding loess into bentonite mud. Improved sand with a bentonite mud injection ratio of a 20% is selected, and the mass ratios of the improved sandy and bentonite are 1 : 3, 2 : 3, and 3 : 3 to adjust the amount of loess. The test results are shown in Table 2. It can be seen from the table that when the mix ratio is 3 : 3, the improved gravelly sand impermeability coefficient reaches 3.47×10^{-5} cm/s, and the slump reaches 160 mm. The addition of loess greatly improves the impermeability of gravelly sand, and the workability is also improved (as shown in Figure 7), thereby meeting the construction needs.

4.2. Ground Reinforcement Method. Grouting reinforcement is an effective method to reduce the ground settlement and ensure that the shield passes through the risk source with strict settlement control requirements [32]. Because ground grouting easily has adverse effects on the original foundation piles under box bridges and there are potential safety hazards, deep grouting of steel pipes is considered to strengthen the soil to control the surface settlement. The permeability of the water-rich sandy layer is good, the water content is large, and the demand for grouting is also large. However, the six grouting holes of the ordinary segment cannot meet the demand, so the segment structure is reformed. As shown in Figure 8, the number of grouting holes can be increased to 16 in each ring on the special segment after the transformation. During construction, the steel flower pipe is driven into the segment grouting hole and then extends out of the segment for 3 m. The 1 : 1 cement water glass double slurry is used to reinforce the soil within 3 m around the segment to meet the larger grouting demand of shield tunneling in the water-rich sand layer.

4.3. Adaptive Transformation Method of the Shield Cutter. The sand soil has poor fluidity and a large friction force. According

(a) Before the improvement (b) After the improvement

Figure 7: The improvement effect of the ballast soil.

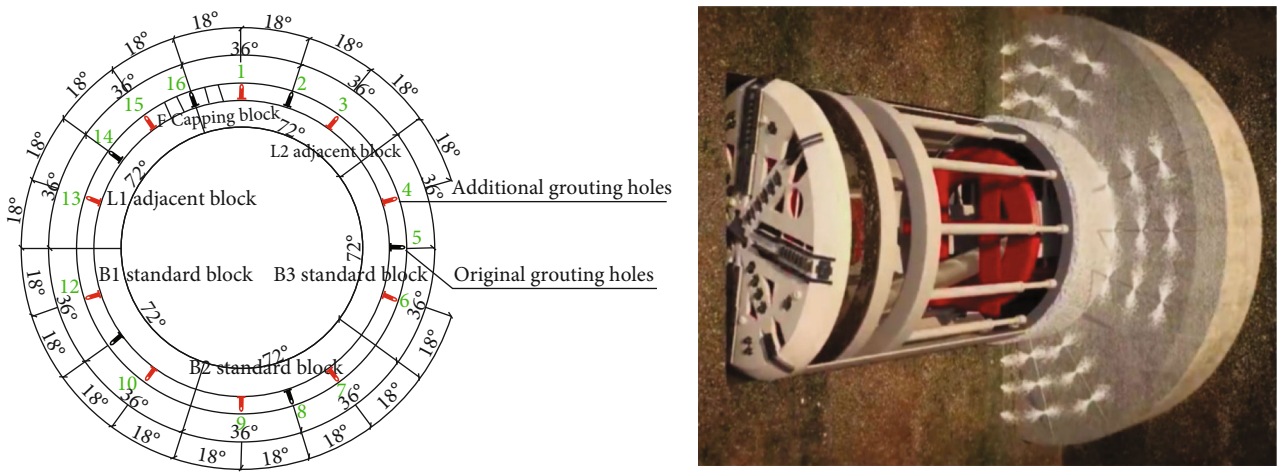

(a) The special segment structure drawing (b) Grouting around segments

Figure 8: The special segment after the transformation.

to the statistics of the wear of the shield cutters in the test zone, it is found that the average wear of the cutters in the left line is 12 mm and that in the right line is 11 mm. According to the geological survey report, the buried depth of shield tunneling under the railway box bridge zone is larger, the standard penetration value of the stratum is higher, and the wear of the shield cutter is expected to be greater. When the traditional tearing knife is used in construction, the friction on both sides is uneven, and it easily fractures, which causes local damage to the tearing knife. This not only reduces the stability of the tearing knife but also aggravates the disturbance of the soil around the shield machine and threatens the safe operation of the railway train above. As shown in Figures 9 and 10, the adaptability of the shield cutter is improved. The protection block is added in the upper, lower, and center to improve the stability of the tearing cutter in use. In addition, the dentate outer wall is arranged on the side of the protection block, and a dumping groove is arranged on the upper protection block to share the cutting pressure of the cutter. The adaptive transformation of the shield cutter not only reduces the damage of uneven friction to the cutter itself and reduces the frequency of replacing the tool but also further reduces the disturbance to the surrounding soil, which is conducive to reducing ground settlement.

5. Rationality Evaluation of the Construction Control Method Based on Monitoring

5.1. Monitoring Scheme. To ensure the construction safety of the tunnel and verify the rationality of the construction control method of shield tunneling under the risk source, the ground settlement and the settlement of the box bridges in the process of shield tunneling under the box bridges are monitored. The layout plan of the monitoring points is shown in Figure 11. A surface settlement monitoring section is set every 5 meters, and the box bridge settlement monitoring points are arranged on the bridge deck. Similarly, a box bridge deck settlement monitoring section is set every 5 meters. To facilitate monitoring, the settlement value of the bridge deck is used to replace the settlement value of the railway to observe the effect of the application of the construction control method.

Shield tunneling construction under railway box bridges is a level I risk source. To quickly obtain more accurate monitoring data, the automatic remote measurement and control system combined with the manual monitoring method is used to observe the deformation of the box bridge deck and surface for 24 hours. As shown in Figure 12(a), the Leica TS50 maglev automatic total station is fixed on the pier of

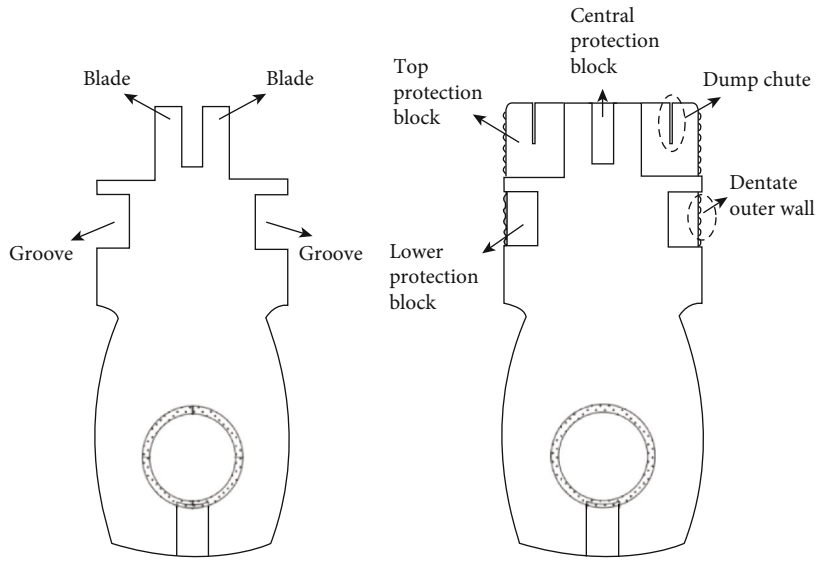

(a) Before the transformation (b) After the transformation

Figure 9: The transformation of the shield tearing cutter.

Figure 10: The new type of the tearing cutter.

the forced alignment, and each measuring point of the box bridge is fixed on the bridge deck of the box bridge with expansion bolts (see Figure 12(b)). The total station transmits the monitoring data to the computer through the CDMA module at a certain time interval, and the monitoring personnel use the computer to transmit the monitoring command to the total station in the remote control room, thereby realizing automatic remote measurement and control.

5.2. Analysis of the Monitoring Results

5.2.1. Settlement Analysis of the Box Bridge Deck. When shield tunneling occurs under the Xibao box bridge and Xicheng box bridge, the settlement data of five typical monitoring sections of the bridge deck are selected for analysis, as shown in Figure 13. Because the two box bridges have four hole box structures, the settlement curve of the bridge deck fluctuates in a zigzag pattern due to the supporting effect of the diaphragm. The bridge deck above the diaphragm easily experiences uplift, and the maximum heave value is 1.9 mm. The maximum settlement of the bridge deck occurs between two diaphragms, which is − 1.9 mm. After adopting the construction control method of shield tunneling under the risk source, the heave and settlement values of the box bridge deck are controlled within ±2 mm, which is far less than the control requirement of ±10 mm stated in the specification. This provides necessary conditions for shield tunneling to safely pass through the Xibao and Xicheng box bridges and demonstrates the rationality and effectiveness of this construction control method.

5.2.2. Analysis of Surface Subsidence. Taking section DB4, section DB7, and section DB10 as the research objects, the surface subsidence data are analyzed. Monitoring focuses on the whole tunneling process of the shield before reaching the risk source, during passing, and after leaving the risk source [33, 34]. As shown in Figure 14, in stage 1, when the shield machine reaches the front of the Xibao box bridge, the ground heave and settlement between the Xibao and Xicheng box bridges are approximately ±0 mm, and the shield has little effect on the ground settlement. In stage 2, in the process of tunneling through the Xibao and Xicheng box bridges, the growth rate of surface settlement increases sharply, and the settlement of section DB4 closer to the Xibao box bridge changes most significantly. With the continuous adjustment and change in the advance speed of the shield machine, the cutter head torque, the cutter head speed, and the chamber pressure, the surface settlement increases slightly. The maximum settlement value occurred in stage 3, which was − 2.1 mm, and the settlement rate slowed down greatly in this stage. Thirty-four days later, the

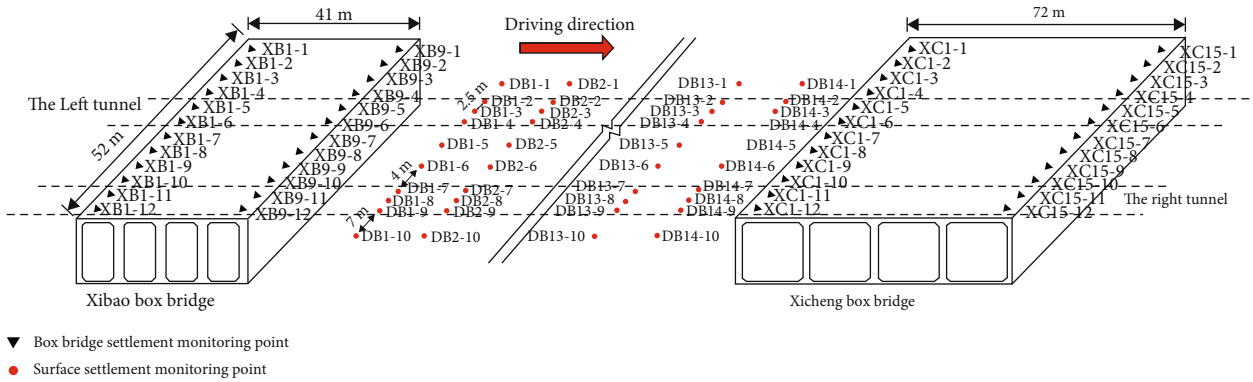

Figure 11: Plane layout of the settlement monitoring points of the ground surface and the box bridges.

(a) The measuring machine (b) The monitoring point prism

Figure 12: The settlement monitoring equipment.

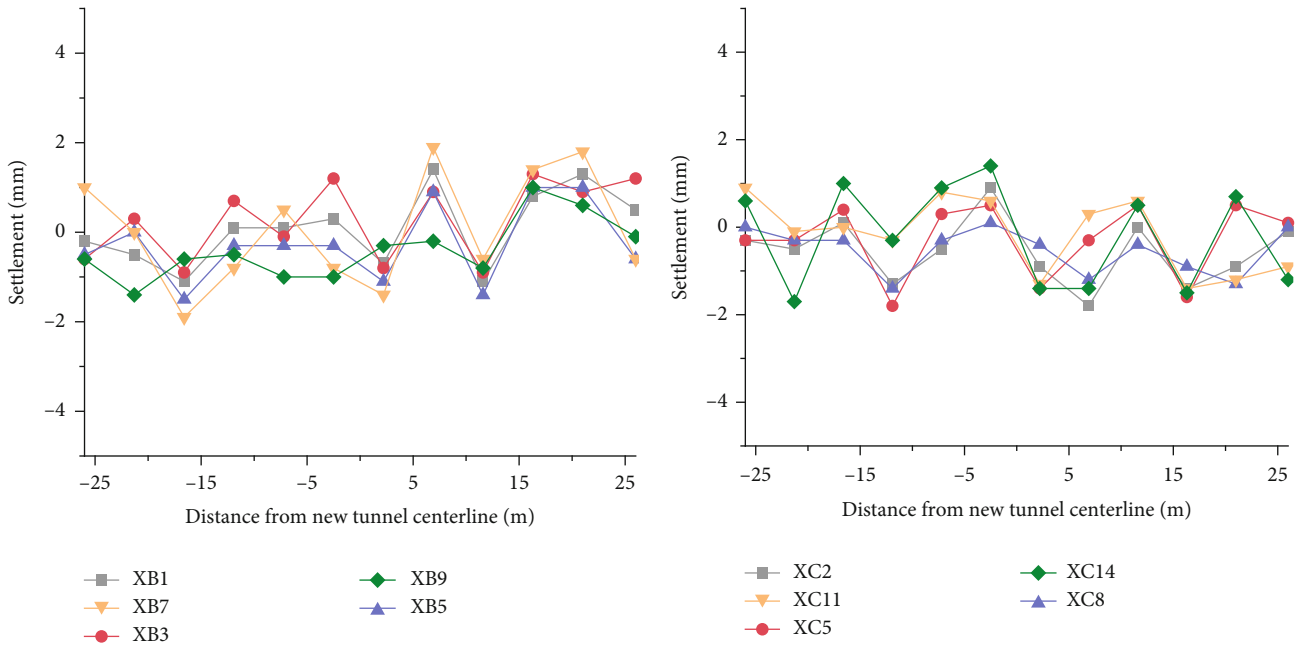

(a) The Xibao box bridge (b) The Xicheng box bridge

Figure 13: The settlement curve of the box bridge deck.

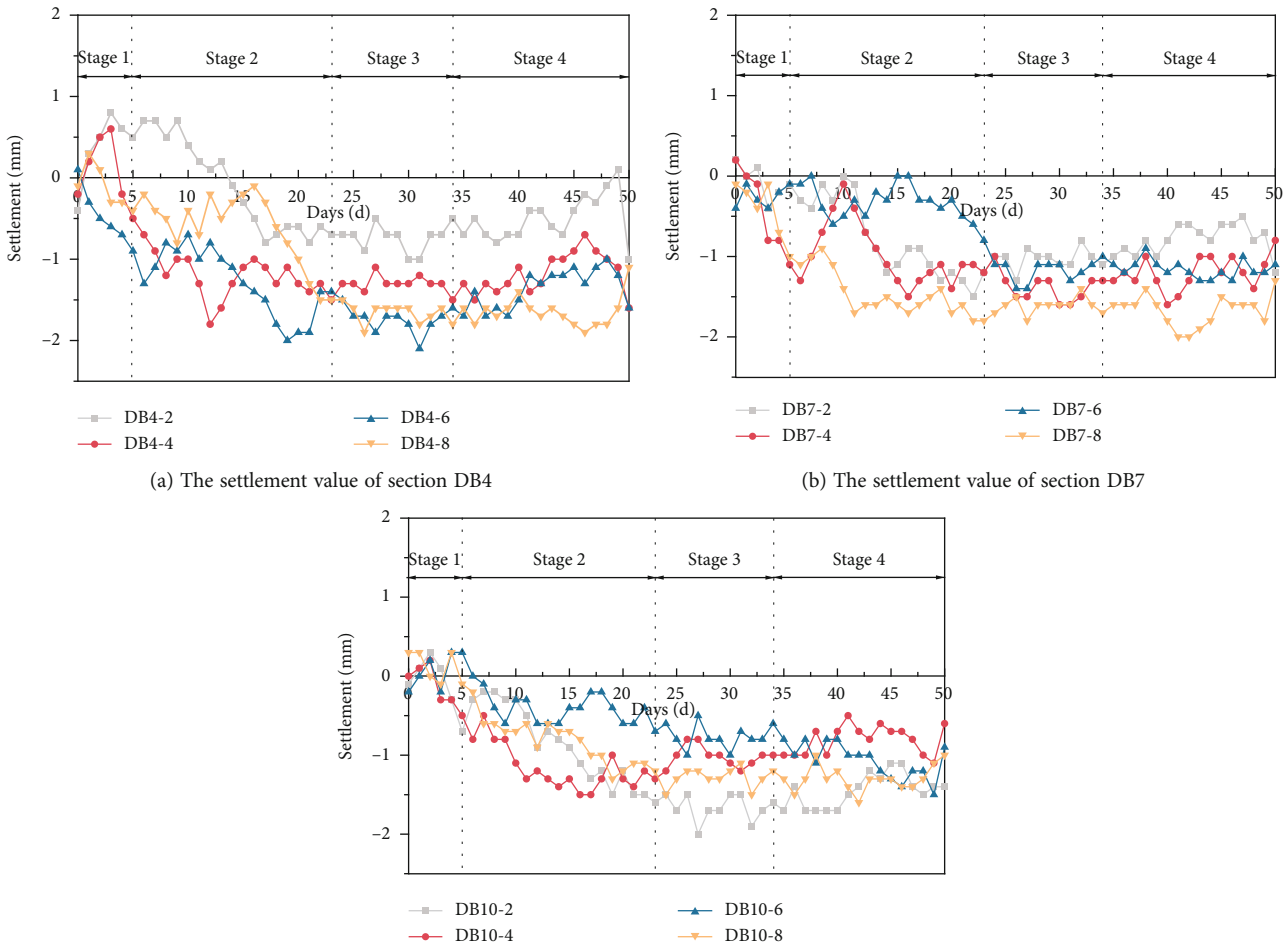

(a) The settlement value of section DB4

(b) The settlement value of section DB7

(c) The settlement value of section DB10

Figure 14: Longitudinal surface subsidence of different monitoring sections.

shield construction of the underpass Xibao and Xicheng box bridges was complete, and the shield machine gradually moved away from the risk source and entered stage 4 of settlement development; at this time, the settlement value tended to be stable. In the whole process of the shield passing through the box bridge, the ground heave and settlement value are controlled within −2.1 mm~0.8 mm; that is, this construction control method can greatly reduce the settlement in the full section water-rich sand layer, which provides the necessary conditions for the safe operation of the train above.

6. Preliminary Determination of a Reasonable Range of Driving Parameters Based on Statistical Analysis

6.1. Analysis of the Influence of the Driving Parameters on the Surface Settlement in the Test Zone. The surface settlement caused by shield tunnel construction is affected by multiple shield tunneling parameters. The rationality of tunneling parameter selection will play a decisive role in surface settlement control, construction quality and efficiency. To optimize the driving parameters, the relationship between the driving parameters and the surface settlement is studied according to the monitoring records of the test zone. The shield machine cuts the soil in front of the face through the cutter head to complete the tunnel excavation and to maintain the stability of the excavation face; it needs to produce a certain soil pressure to balance the water and soil pressure of the excavation face. Based on this, the advance speed, cutter head torque, cutter head speed, and chamber pressure are selected as the key parameters of tunneling. As shown in Figure 15, the maximum value, minimum value, and average value of surface settlement corresponding to different driving parameters are counted, and the change trend of surface deformation under the influence of key driving parameters is analyzed. S_{Lmin} is the minimum value, S_{Lmax} is the maximum value, S_{Lavg} is the average value of the left line, S_{Rmin} is the minimum value, S_{Rmax} is the maximum value, and S_{Ravg} is the average value of the right line.

In the process of driving in the test zone, the range of surface heave and settlement is −18.1 mm~2.6 mm. The advance speed of the shield machine is mainly controlled between 70 and 115 mm/min. With the increase in the advance speed, the disturbance of the shield machine to the soil increases correspondingly, and the surface

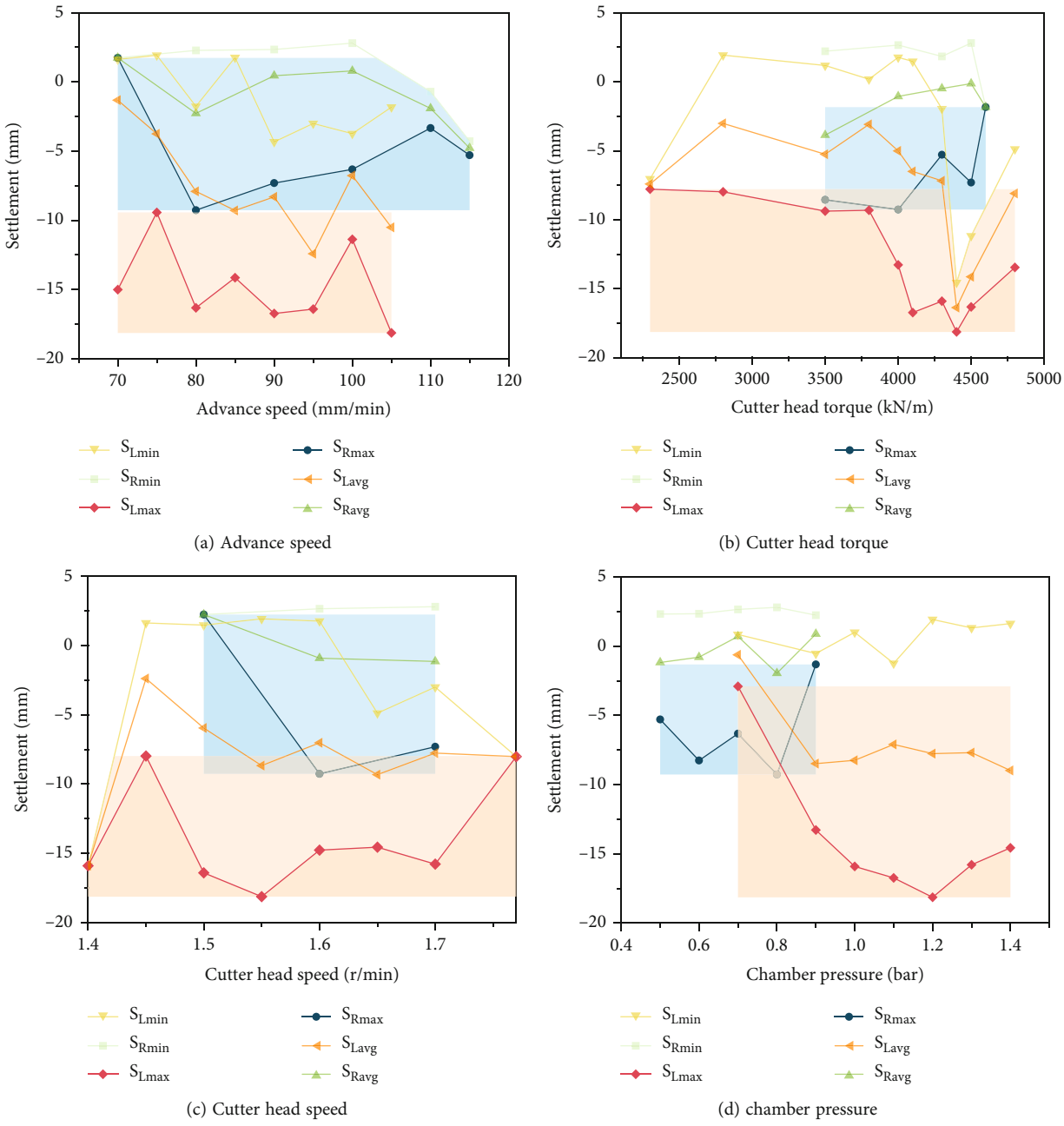

Figure 15: Relationship between surface settlement and driving parameters.

settlement S_{Lavg} and S_{Ravg} caused by the left and right line shields also increase. The high-speed tunneling state is unfavorable, and more precise requirements are introduced for the control of shield machine propulsion equipment, excavation equipment, grouting equipment, etc., which easily increases the construction risk. Therefore, the advance speed should be reduced to maintain the stability of excavation. The variation in the cutter head torque is large, the minimum value is 2300 kN/m, and the maximum value is 4800 kN/m. When the cutter head torque value reaches 3750 kN/m, with the increase of cutter head torque, the growth rate of the surface settlement value S_{Lavg} increases sharply. When the cutter head torque increases to approximately 4400 kN/m, S_{Lavg} reaches a maximum, and then the surface settlement value decreases with increasing cutter head torque. As shown in Figure 15, the rotation speed of the cutter head is maintained between 1.5 and 1.7 r/min. When the rotation speed of the cutter head is less than 1.5 r/min, the surface settlement values S_{Lavg} and S_{Ravg} are relatively small and are maintained within 5 mm. When the rotation speed of the cutter head is greater than 1.5 r/min, the surface settlement values S_{Lavg} and S_{Ravg} begin to increase and finally fluctuate at approximately 10 mm. This is mainly because the faster the cutter head speed is, the stronger the cutting capacity of the cutter head to the soil and the greater the disturbance to the surrounding strata, while the settlement

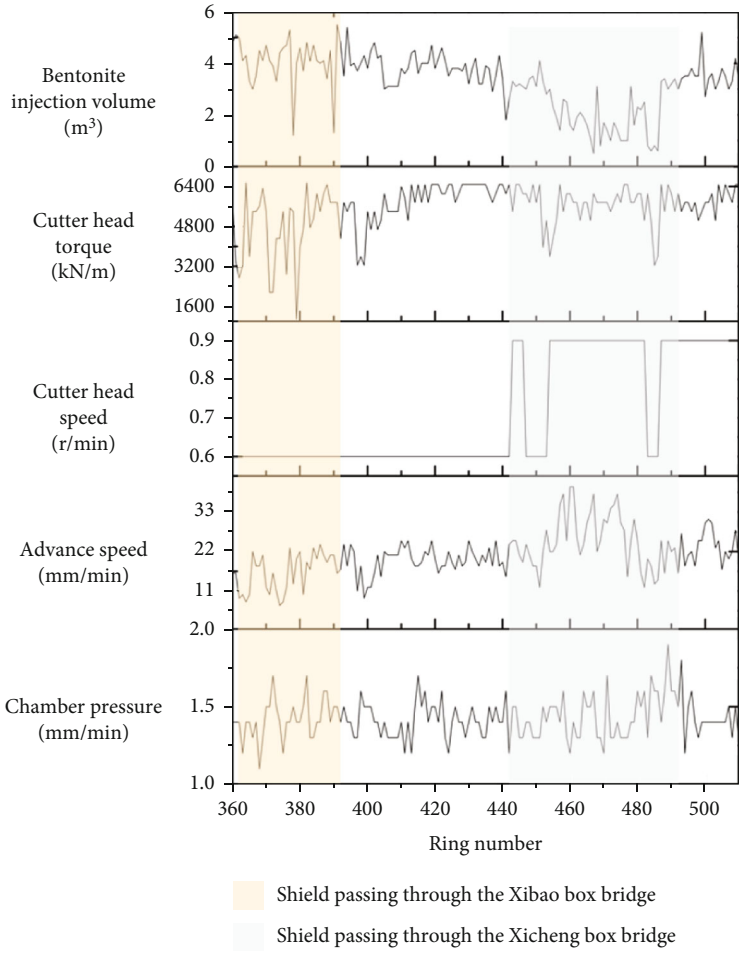

Figure 16: Driving parameters of shield tunneling under box bridges.

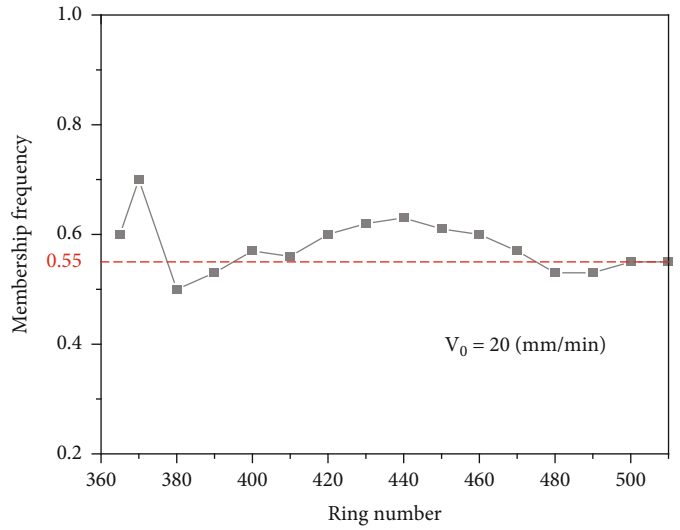

Figure 17: Membership frequency related to the "reasonable advance speed" of 20 mm/min.

increases. Therefore, to reduce the risk of shield construction, the cutter head speed should be properly controlled to prevent it from being too high. In Figure 15(d), the chamber pressure during the excavation of the right tunnel is between 0.5 and 0.9 bar, and during the excavation of the left tunnel is between 0.7 and 1.4 bar. The fluctuation of the chamber pressure in the right tunnel is small, and the surface settlement caused by the chamber pressure S_{Ravg} is smaller

Table 3: Optimum control range of the driving parameters.

Driving parameters	Optimum control range
Cutter head torque	5760~6120 (kN/m)
Cutter head speed	0.6~0.9 (r/min)
Chamber pressure	1.3~1.5 (bar)
Bentonite injection volume	1.4~3.8 (m^3)
Advance speed	20~21 (mm/min)

than S_{Lavg}, which indicates that the smaller and more stable chamber pressure in the water-rich sand layer is conducive to the control of the surface settlement.

In the actual process of shield tunneling, many factors affect the surface settlement, and the relationship between them and the driving parameters is complex, so it is difficult to conform to a certain variation law. However, the fluctuation range of the driving parameters and the influence trend on the surface settlement can provide some reference for the optimization of driving parameter control in the process of shield tunneling in a water-rich sand layer.

6.2. Analysis of the Driving Parameters of Shield Tunneling under Risk Sources. The settlement control of shield tunneling under the railway box bridge is ideal, which is inseparable from the reasonable control of the driving parameters. Figure 16 shows the driving parameters recorded during the construction of the left line tunnel. To reduce the ground settlement and control the driving attitude, the advance speed of shield tunneling under the box bridge is reduced compared with the test zone. After ring 440, with increasing cutter head speed, the advance speed increases from 20 mm/min to 30 mm/min, which indicates that the different stratum conditions have a certain impact on the advance speed of the shield machine. Compared with the gravelly sand stratum, when driving in the medium sand stratum with relatively large standard penetration, the cutter head speed is relatively low, and the driving speed is slow. Based on the analysis of the cutter head speed in the test zone, the cutter head speed is reduced to reduce the soil settlement. Before the 440 ring, the cutter head speed is constant at 0.6 r/min under the setting of the construction personnel. When the shield machine approaches the Xicheng box bridge, the stratum condition changes from medium sand to gravel sand, and the cutter head speed increases to 0.9 r/min. The change in the chamber pressure is small, and it is stable between 1.1 and 1.7 bar. The cutter head torque data have high discreteness, and the variation law is consistent with that of the bentonite injection data, which indicates that the soil improvement effect has a great influence on the cutter head torque and the uneven size of the soil blocks cut by the shield machine makes the cutter head torque fluctuate more easily. Compared with the test zone, the cutter head torque increases obviously, which may be due to the following two reasons: One reason is that the depth of this zone is deep, which makes the friction torque between the cutter head and soil larger; the other is that the penetration of the cutter head in this zone is larger, which makes the resistance of the stratum larger when cutting.

6.3. Statistical Test of the Driving Parameters. According to fuzzy set theory [35], a fuzzy statistical test is carried out on the driving parameter data of shield tunneling under box bridges in a full section water-rich sand layer to analyze and obtain the reasonable driving parameters range for the shield machine.

The advance speed is an overall reflection of the tunneling situation of the shield machine. Taking the advance speed as an example, the statistical test takes $V = [0.50]$ mm/min as the domain of the advance speed. Fuzzy set A represents the fuzzy concept for a "reasonable driving speed." To determine the membership degree of a fixed driving speed to A, the membership frequency f is calculated. As shown in Figure 17, taking the driving speed $v_0 = 20$ mm/min as an example, the membership frequency f of the "reasonable driving speed" of the shield is stable at approximately 0.55 with the increase in the number of samples, so $A(v_0) = A(20) = 0.55$ can be applied. Similarly, the membership frequency f of other fixed driving speeds to the "reasonable driving speed" can be obtained. In the monitoring data of this test, the minimum driving speed is 5 mm/min, and the maximum driving speed is 40 mm/min, which can take 4.5 mm/min as the starting point and 40.5 mm/min as the ending point. The driving speed [4.5,40.5] mm/min is divided into 46 small areas with a length of 1 mm/min, and each small area is represented by the median value to calculate the membership frequency and obtain the membership frequency. The calculation results are shown in Table 3.

By calculating the membership frequency related to the advance speed, the membership frequency histogram is drawn as shown in Figure 18(a). The graph is continuously depicted, that is, the membership function curve is obtained. The membership function approximately obeys the Gaussian distribution, and the correlation coefficient is 0.95. The fitting is good. In the theory of fuzzy sets, the element v whose membership frequency is greater than 0 is called the support set of fuzzy set A, denoted as suppA, and the element whose membership frequency is greater than α is called the α cut set of fuzzy set A, denoted as A_α. To obtain a reasonable value range for the advance speed, the confidence level $\alpha = 0.5$ is selected [36], that is, the advance speed when the membership frequency is greater than 0.5 is the reasonable value range of the advance speed, in this project: $A_\alpha = \{20, 21\}$. In the same way, the reasonable range of the other driving parameters, such as the cutter head torque, cutter head speed, chamber pressure, and bentonite grouting volume, can also be determined by the above fuzzy statistical test method. The membership frequency histogram is shown in Figures 18(b)–18(d), and the specific numerical range calculated is shown in Table 3.

The results of the fuzzy statistical test are obtained by mathematical analysis based on the measured data. Through the analysis and statistical testing of the driving parameters of shield tunneling under box bridges, a reasonable control range of the cutter head torque, cutter head speed, chamber pressure, bentonite injection volume, and advance speed is

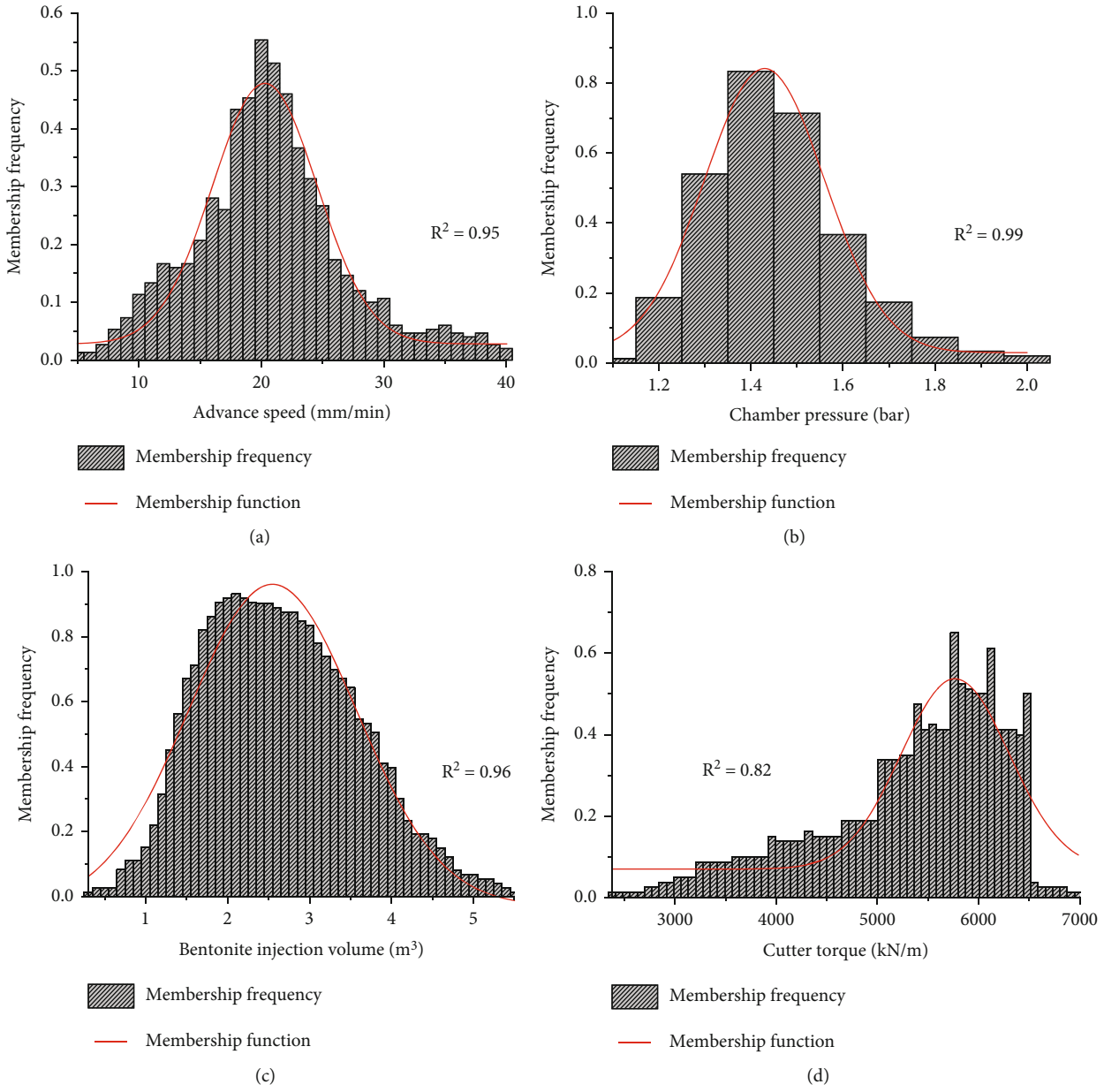

Figure 18: The membership frequency and the membership function of the driving parameters.

proposed when shield tunneling is performed under a risk source in a full section water-rich sand layer to provide a reference for similar projects.

7. Conclusions

This paper introduces the construction control method combining soil improvement, stratum reinforcement, and shield machine adaptive transformation, which can effectively reduce the disturbance of water-rich sand layer caused by tunnel construction, ensure the railway operation safety when the shield is constructed, and have good social and economic benefits. The main conclusions are as follows:

(1) When the EPB shield machine is used in the water-rich sand layer, sodium bentonite with an expansion time of 18 h and a concentration of 10% should be used as the improver. After driving through the gravelly sand layer, the improvement effect of this modifier is not ideal. After adding 50% loess into the bentonite slurry, the impermeability of gravelly sand is greatly improved, the workability is obviously improved, and the improvement effect is good. The effect of surface settlement control in the water-rich sand layer can be improved by using special segments with grouting holes for the secondary grouting reinforcement of the surrounding soil and adding protective blocks for shield cutters

(2) There is a great correlation between the surface settlement and the driving speed in shield tunneling, and appropriately reducing the driving speed is

conducive to reducing the surface settlement; different stratum conditions have a certain impact on the driving parameters. Compared with the gravelly sand stratum, when driving in the medium sand stratum with larger standard penetration, the driving speed is slower, and the cutter head speed is lower; the change in cutter head torque is greatly affected by the bentonite injection volume, and the fluctuation law is consistent with the injection volume of bentonite

(3) Based on the statistical analysis of the driving parameters of shield tunneling under railway box bridges, a reasonable range of driving parameters is proposed, which provides a reference for the control of driving parameters when shield tunneling is under a risk source in a similar adverse stratum and reduces the increase in surface settlement caused by the individual experience. However, since the reasonable value range is calculated based on this project, its applicability needs to be further verified and improved in future engineering practice

Data Availability

All data, models, and code generated or used during the study appear in the submitted article.

Conflicts of Interest

The authors declare that they have no known competing financial interests or personal relationships that could have appeared to influence the work reported in this paper.

Authors' Contributions

Yuan Mei contributed to the conceptualization, funding acquisition, methodology, and supervision. Xinyue Zhang contributed to the data curation, formal analysis, writing-original draft, visualization, and investigation. Shumin Zhang contributed to the data curation. Rong Wang and Tong Yang contributed to the resources. Yuhang Zhang contributed to the validation.

Acknowledgments

This project was supported by the National Natural Science Foundation of China (No. 51408463) and the Key R&D Projects in Shaanxi Province (No. 2020SF-373).

References

[1] Y. Liang, X. Chen, J. Yang, J. Zhang, and L. Huang, "Analysis of ground collapse caused by shield tunnelling and the evaluation of the reinforcement effect on a sand stratum," *Engineering Failure Analysis*, vol. 115, article 104616, 2020.

[2] X. Y. Wang, Z. Ma, and Y. T. Zhang, "Research on safety early warning standard of large-scale underground utility tunnel in ground fissure active period," *Frontiters in Earth Science*, vol. 10, article 828477, 2022.

[3] X. Wang, Q. Song, and H. Gong, "Research on deformation law of deep foundation pit of station in core region of saturated soft loess based on monitoring," *Advances in Civil Engineering*, vol. 2022, Article ID 848152, 16 pages, 2022.

[4] P. A. Ferreira and A. López-Pita, "Numerical modelling of high speed train/track system for the reduction of vibration levels and maintenance needs of railway tracks," *Construction and Building Materials*, vol. 79, pp. 14–21, 2015.

[5] A. K. L. Kwong, C. C. W. Ng, and A. Schwob, "Control of settlement and volume loss induced by tunneling under recently reclaimed land," *Underground Space*, vol. 4, no. 4, pp. 289–301, 2019.

[6] A. Sirivachiraporn and N. Phienwej, "Ground movements in EPB shield tunneling of Bangkok subway project and impacts on adjacent buildings," *Tunnelling and Underground Space Technology*, vol. 30, pp. 10–24, 2012.

[7] X. Y. Xie, Y. B. Yang, and M. Ji, "Analysis of ground surface settlement induced by the construction of a large- diameter shield-driven tunnel in Shanghai, China," *Tunnelling and Underground Space Technology*, vol. 51, pp. 120–132, 2016.

[8] C. Zhu, "Control of surface settlement by considering shield tunneling technology," *KSCE Journal of Civil Engineering*, vol. 21, no. 7, pp. 2896–2907, 2017.

[9] X. T. Lin, R. P. Chen, H. N. Wu, and H. Z. Chen, "Three-dimensional stress-transfer mechanism and soil arching evolution induced by shield tunneling in sandy ground," *Tunnelling and Underground Space Technology*, vol. 93, article 103104, 2019.

[10] B. Bai, Q. Nie, Y. Zhang, X. Wang, and W. Hu, "Cotransport of heavy metals and SiO_2 particles at different temperatures by seepage," *Journal of Hydrology (Amsterdam)*, vol. 597, article 125771, 2021.

[11] B. Bai, R. Zhou, G. Cai, W. Hu, and G. Yang, "Coupled thermo-hydro-mechanical mechanism in view of the soil particle rearrangement of granular thermodynamics," *Computers and Geotechnics*, vol. 137, p. 104272, 2021.

[12] H. Sohaei, M. Hajihassani, E. Namazi, and A. Marto, "Experimental study of surface failure induced by tunnel construction in sand," *Engineering Failure Analysis*, vol. 118, article 104897, 2020.

[13] G. L. Ye, T. Hashimoto, S. L. Shen, H. H. Zhu, and T. H. Bai, "Lessons learnt from unusual ground settlement during double-O-tube tunnelling in soft ground," *Tunnelling and Underground Space Technology*, vol. 49, pp. 79–91, 2015.

[14] J. Lai, H. Zhou, K. Wang et al., "Shield-driven induced ground surface and Ming Dynasty city wall settlement of Xi'an metro," *Tunnelling and Underground Space Technology*, vol. 97, article 103220, 2020.

[15] R. P. Chen, X. T. Lin, X. Kang et al., "Deformation and stress characteristics of existing twin tunnels induced by close-distance EPBS under-crossing," *Tunnelling and Underground Space Technology*, vol. 82, pp. 468–481, 2018.

[16] Z. Wang, K. W. Zhang, G. Wei, B. Li, Q. Li, and W. J. Yao, "Field measurement analysis of the influence of double shield tunnel construction on reinforced bridge," *Tunnelling and Underground Space Technology*, vol. 81, pp. 252–264, 2018.

[17] B. Yuan, Z. Li, Y. Chen et al., "Mechanical and microstructural properties of recycling granite residual soil reinforced with glass fiber and liquid-modified polyvinyl alcohol polymer," *Chemosphere*, vol. 286, article 131652, Part 1, 2022.

[18] B. Yuan, Z. Li, W. Chen et al., "Influence of groundwater depth on pile–soil mechanical properties and fractal characteristics under cyclic loading," *Fractal and Fractional*, vol. 6, no. 4, p. 198, 2022.

[19] Z. Li, Z. Q. Chen, L. Wang, Z. Zeng, and D. Gu, "Numerical simulation and analysis of the pile underpinning technology used in shield tunnel crossings on bridge pile foundations," *Underground Space*, vol. 6, no. 4, pp. 396–408, 2020.

[20] B. Liu, D. H. Xi, and P. Xu, "Study on the interaction of metro shield tunnel construction under-crossing the existing Longhai railway," *Geotechnical and Geological Engineering*, vol. 38, no. 2, pp. 2159–2168, 2020.

[21] B. Zhao, X. Wang, C. Zhang, W. Li, R. Abbassi, and K. Chen, "Structural integrity assessment of shield tunnel crossing of a railway bridge using orthogonal experimental design," *Engineering Failure Analysis*, vol. 114, article 104594, 2020.

[22] W. P. Qian, T. Y. Qi, Y. J. Zhao, Y. Z. Le, and H. Y. Yi, "Deformation characteristics and safety assessment of a high-speed railway induced by undercutting metro tunnel excavation," *Journal of Rock Mechanics and Geotechnical Engineering*, vol. 11, no. 1, pp. 88–98, 2019.

[23] G. Zheng, Q. Fan, T. Q. Zhang et al., "Multistage regulation strategy as a tool to control the vertical displacement of railway tracks placed over the building site of two overlapped shield tunnels," *Tunnelling and Underground Space Technology*, vol. 83, pp. 282–290, 2019.

[24] N. A. Do, D. Dias, P. Oreste, and I. Djeran-Maigre, "Three-dimensional numerical simulation of a mechanized twin tunnels in soft ground," *Tunnelling and Underground Space Technology*, vol. 42, pp. 40–51, 2014.

[25] M. Kavvadas, D. Litsas, I. Vazaios, and P. Fortsakis, "Development of a 3D finite element model for shield EPB tunnelling," *Tunnelling and Underground Space Technology*, vol. 65, pp. 22–34, 2017.

[26] A. Lambrughi, L. M. Rodriguez, and R. Castellanza, "Development and validation of a 3D numerical model for TBM-EPB mechanised excavations," *Computers and Geotechnics*, vol. 40, no. 1, pp. 97–113, 2012.

[27] X. Y. Hu, C. He, Z. Z. Peng, and W. B. Yang, "Analysis of ground settlement induced by earth pressure balance shield tunneling in sandy soils with different water contents," *Sustainable Cities and Society*, vol. 45, pp. 296–306, 2019.

[28] B. Yuan, Z. Li, Z. Zhao, H. Ni, Z. Su, and Z. Li, "Experimental study of displacement field of layered soils surrounding laterally loaded pile based on transparent soil," *Journal of Soils and Sediments*, vol. 21, no. 9, pp. 3072–3083, 2021.

[29] H. Huang, C. Wang, J. Dong, J. Zhou, J. Yang, and Y. Li, "Conditioning experiment on sand and cobble soil for shield tunneling," *Tunnelling and Underground Space Technology*, vol. 87, pp. 187–194, 2019.

[30] Q. Xu, L. Zhang, H. Zhu, Z. Gong, J. Liu, and Y. Zhu, "Laboratory tests on conditioning the sandy cobble soil for EPB shield tunnelling and its field application," *Tunnelling and Underground Space Technology*, vol. 105, article 103512, 2020.

[31] B. Bai, Y. Wang, D. Rao, and F. Bai, "The effective thermal conductivity of unsaturated porous media deduced by pore-scale SPH simulation," *Frontiers in Earth Science (Lausanne)*, vol. 10, 2022.

[32] X. Xie, J. Zhai, and B. Zhou, "Back-fill grouting quality evaluation of the shield tunnel using ground penetrating radar with bi-frequency back projection method," *Automation in Construction*, vol. 121, article 103435, 2021.

[33] D. Dias and R. Kastner, "Movements caused by the excavation of tunnels using face pressurized shields – analysis of monitoring and numerical modeling results," *Engineering Geology*, vol. 152, no. 1, pp. 17–25, 2013.

[34] G. Zheng, P. Lu, and Y. Diao, "Advance speed-based parametric study of greenfield deformation induced by EPBM tunneling in soft ground," *Computers and Geotechnics*, vol. 65, pp. 220–232, 2015.

[35] L. A. Zadeh, "Probability measures of fuzzy events," *Journal of Mathematical Analysis and Applications*, vol. 23, no. 2, pp. 421–427, 1968.

[36] P. Lu, G. Zheng, H. Y. Lei, and W. J. Zhang, "Statistical experiment and optimal control on driving parameters in shield tunnel," *Journal of Tianjin University (Science and Technology)*, vol. 49, no. 10, pp. 1062–1070, 2016.